DEVELOPMENT OF A NEW LIMIT STATE FUNCTION FOR THE FAILURE OF PIPELINES DUE TO MECHANICAL DAMAGE

A Francis[1], C S Jandu[1], R M Andrews[2*], T J Miles[2], V Chauhan [2]

1 AFAA, EPOS House, Ripley, Derbyshire, DE5 3GH
2 Advantica, Ashby Road, Loughborough, Leicestershire, LE11 3GR

* Presenting Author; bob.andrews@advantica.biz

ABSTRACT

It is widely accepted that mechanical damage is one of the major causes of the failure of high pressure steel pipelines. A mechanistic model that would predict when failure of a pipeline would occur due to combined dents and gouges would facilitate better management of this risk. This can be expressed as a limit state function where the driving force for failure is compared with the resistance of the structure. In the UK a limit state function was developed in the early 1980s based on the fracture mechanics methods available at that time. Although this model had some empirical constants calibrated into it, a major feature was that it had a mechanistic basis, rather than being a simple curve fit.

In the intervening period since the original analysis, there have been major developments in both fracture mechanics techniques and in the understanding of the factors which influence the behaviour of pipeline defects. There is also increasing regulatory pressure to improve the management of the risks associated with pipelines. Hence Advantica was commissioned by UKOPA, the United Kingdom Onshore Pipelines Association, to develop an improved limit state function which would address some of the perceived shortcomings of the original model. This paper presents the results of the initial stages of this development work. The major enhancements are:

- Alignment with the latest version of the R6 defect assessment procedures
- Inclusion of residual stresses resulting from the denting process
- Representation of the gouge as a stress raiser with a micro-cracked layer at the base

It is shown that these developments give an improved prediction of the original data set used to develop the model and should provide a good basis for further developments.

1 INTRODUCTION

It has been recognised for many years that external interference, typically from excavating equipment, can pose a serious threat to the structural integrity of high pressure onshore pipelines. The most onerous scenario possible is an impact resulting in damage of sufficient severity to cause a full-bore rupture of the pressurised pipeline. This would lead to the rapid release of a large quantity of gas which, if ignited, could pose a very significant safety hazard to anyone in the vicinity of the release.

In recognition of this, comprehensive integrity and risk management procedures are customarily adopted by pipeline operators. These procedures comprise a number of mitigating measures that generally include:

- management of the likelihood of impact
  - surveys and surveillance
  - burial depth
  - third party liaison (landowner contact, one-call systems) and supervision of third party activities close to the pipeline
- management of the likelihood of rupture if impact occurs
  - maximum design factor
  - minimum wall thickness
- management of the safety hazard if a rupture occurs
  - minimum separation distance between the pipeline and occupied buildings
  - allowable population density

Thus, in basic terms, the probability of occurrence of a safety hazard, $p(S)$, can be expressed as

$$p(S) = p(S \mid R)\,p(R \mid I)\,p(I) \qquad (1)$$

where $p(S \mid R)$ is the probability of a safety hazard given that a rupture has occurred, $p(R \mid I)$ is the probability of a rupture given that an impact has occurred and $p(I)$ is the probability of occurrence of an impact. Although simplistic, this expression serves to illustrate that the risk management procedure comprises three basic elements and consequently that due consideration should be given to each of these.

Over recent years extensive experimental and theoretical research work has been undertaken within the UK to construct sophisticated models for determining the quantity $p(S \mid R)$ and these models form the 'hub' of the risk assessment software PIPESAFE [1].Statistically significant data have been collected over many years for the UK gas transmission system to quantify the likelihood of impact, $p(I)$; the majority of impacts do not result in failure. On the other hand the quantity $p(R \mid I)$ is based on fracture mechanics formulations that were originally developed around 1980 [2] and subsequently modified by EPRG [3]. It is therefore 'behind the times' when compared with its two counterparts in equation (1). This does not mean that the existing formulation is 'unsafe' (there has not been a full bore rupture within the UK in over 500,000 kilometre years of high pressure pipeline operation), however, there are important issues to be considered. These are:

- Fracture mechanics methods have improved considerably over the past 25 years
- A mechanistic model is a better basis for developing an understanding of the problem than a statistical fit to parameters [4]
- The UK Health and Safety Executive (HSE) adopt a different (more up-to-date) method [5]
- Some pipelines in the UK are being operated more onerously than previously (uprating)
- The model is a major component in the management of risk and land use planning associated with pipelines

In view of the above, the United Kingdom Onshore Pipelines Association (UKOPA) have commissioned Advantica to undertake a theoretical study to update the current fracture mechanics formulation (limit state function), on which $p(R \mid I)$ is based. The study had the objectives of,

- achieving alignment with contemporary fracture mechanics methods
- achieving alignment with the HSE method

As with all theoretical work of this nature, there is a requirement for some experimental work for the purpose of validation. For the present purpose the approach adopted is to use the test data set that was used when developing the original limit state function [2]. However, although extensive testing was undertaken (132 tests) some of the data are incomplete or (for the present purpose) missing. In view of this, whilst meeting the above objectives, the outcome of the present work will form the basis of a more extensive future work program incorporating more detailed testing.

This report describes the general fracture mechanics approach that has been adopted and identifies the relationship between this approach and the original model. It then goes on to derive the new model, incorporating a number of new features, and illustrates the fit of the new model to the original test data.

2 THE ELASTIC-PLASTIC FRACTURE MECHANICS METHODOLOGY

The methodology to be adopted recognises that a steel structure, containing a sharp, crack like defect, can generally fail due to a combination of plastic collapse and fracture. The salient features of this methodology are described below and are also documented in published standards [6], [7] for further reference.

2.1 Fracture

Failure due to fracture is predicted to occur if the inequality,

$$K_r \geq 1 \tag{2}$$

is satisfied, where the parameter K_r is defined as

$$K_r = \frac{(K_m^p + K_m^s + K_b^p + K_b^s)}{K_{mat}} + \rho \,. \tag{3}$$

In the above, the parameter ρ is known as the plasticity correction factor and K_m^p, K_m^s, K_b^p and K_b^s are measures of the stress singularity that occurs at the sharp front of a crack-like defect, in a loaded structure due to various categories of stress. They are known as the primary membrane, secondary membrane, primary bending and secondary bending stress intensity factors, respectively. The plasticity correction factor is introduced to take account of the increased driving force for fracture due to interactions between the contributions due to the primary and secondary stresses.

The parameter, K_{mat}, is a material property, known as the fracture toughness and is a measure of the material resistance to fracture. For the present analysis no distinction is drawn between brittle (cleavage) or ductile tearing fracture. In the pipeline industry it is not common to measure the fracture toughness directly but rather to determine it using a correlation with the Charpy energy, C_V. The correlation was expressed as

$$K_{mat} = AC_v^{\alpha} + B \tag{4}$$

where A, B and α are empirical constants. These formulations are discussed in more detail later.

2.2 Plastic Collapse

Failure due to plastic collapse of the remaining ligament is predicted to occur if the inequality,

$$S_r \geq 1\,, \tag{5}$$

is satisfied, where the collapse ratio S_r is defined by

$$S_r = \frac{\sigma_{ref}}{\sigma_f}\,. \tag{6}$$

In the above σ_{ref} is a measure of the stress state in the ligament ahead of the defect and is known as the reference stress. The parameter σ_f is a material property known as the flow stress and is a measure

of the resistance of the material to plastic collapse which recognises the effects of work hardening. A general definition of flow stress is given by

$$\sigma_f = \lambda\sigma_y + (1-\lambda)\sigma_u \tag{7}$$

where σ_y is the yield strength, σ_u the ultimate tensile strength and λ is a dimensionless scalar quantity lying within the range zero to unity. Each of the above terms is discussed in more detail later.

2.3 Elastic-Plastic Fracture

In general, the failure of steel structures containing crack like defects will occur due to a combination of fracture and plastic collapse. In recognition of this, the above two inequalities are combined and expressed in the form

$$K_r \geq F(S_r) \quad , \qquad S_r \leq 1 \, , \tag{8}$$

where F is a function that decreases monotonically from unity to zero as S_r increases from zero to unity. The failure mechanism governed by the above inequality is known as elastic-plastic fracture and the curve described by the function F is known as the failure assessment line. Qualitatively, the failure assessment line describes the increased driving force for fracture that occurs as a result of plasticity. The value of K_r is irrelevant for $S_r > 1$ since failure will necessarily occur due to plastic collapse as described by inequality (5).

2.4 Overview

Based on the above, it is noted that the limit state function comprises the following items:

- the failure assessment line, $F(S_r)$
- the reference stress, σ_{ref}
- the stress intensity factors, K_m^p, K_m^s, K_b^p and K_b^s
- the plasticity correction term, ρ
- the flow stress, σ_f
- the correlation between fracture toughness, K_{mat} and Charpy energy, C_v

In Section 3 the specific details of each of the above items that are relevant to the existing limit state function, [2], [3] are described. In Section 4 the changes to a number of the formulations are introduced in order to produce a new limit state function (based on contemporary fracture mechanics methods) that is aligned to the limit state function used by HSE [3].

3 THE EXISTING LIMIT STATE MODEL

A brief description of the salient features of a generalized fracture mechanics approach to assessing the significance of defects in loaded structures has been provided in Section 2. The specific formulations of each of the key elements of the approach that are relevant to the current model [2], [3] are described in this section.

3.1 The Damage

It is assumed that external interference causes a dent containing a gouge in the wall of the pipe; see Figure 1. The limit state function, described in this section, is thus used to determine the conditions for failure of a gouge of depth a and length L located in a dent of depth D that is present in a pipeline having radius R, wall thickness w, yield strength σ_y, ultimate tensile strength, σ_u, Charpy toughness C_v and subject to internal pressure P. See Figure 1 for details.

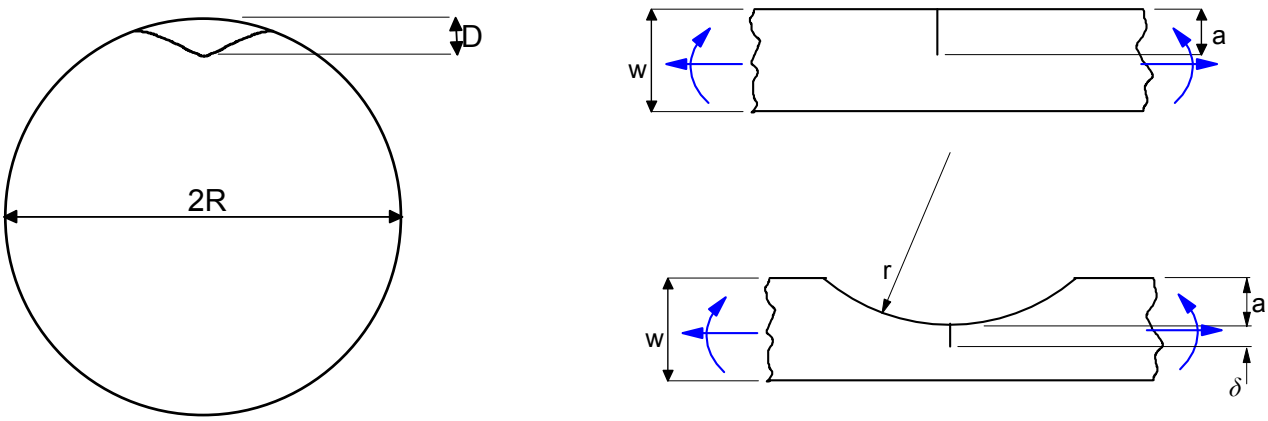

Figure 1 Dent gouge model details. Left – pipe with a dent; top right – gouge modelled as a straight crack subject to membrane and bending stress; bottom right – gouge with a radius and a microcrack.

3.2 The Failure Assessment Line

The functional form of F was based on the Dugdale[7] strip yield model and is given by

$$F = S_r \left[\frac{8}{\pi^2} \ln \sec\left(\frac{\pi}{2} S_r \right) \right]^{-\frac{1}{2}}. \qquad (9)$$

A plot of the function described by equation (9) is shown in Figure 2.

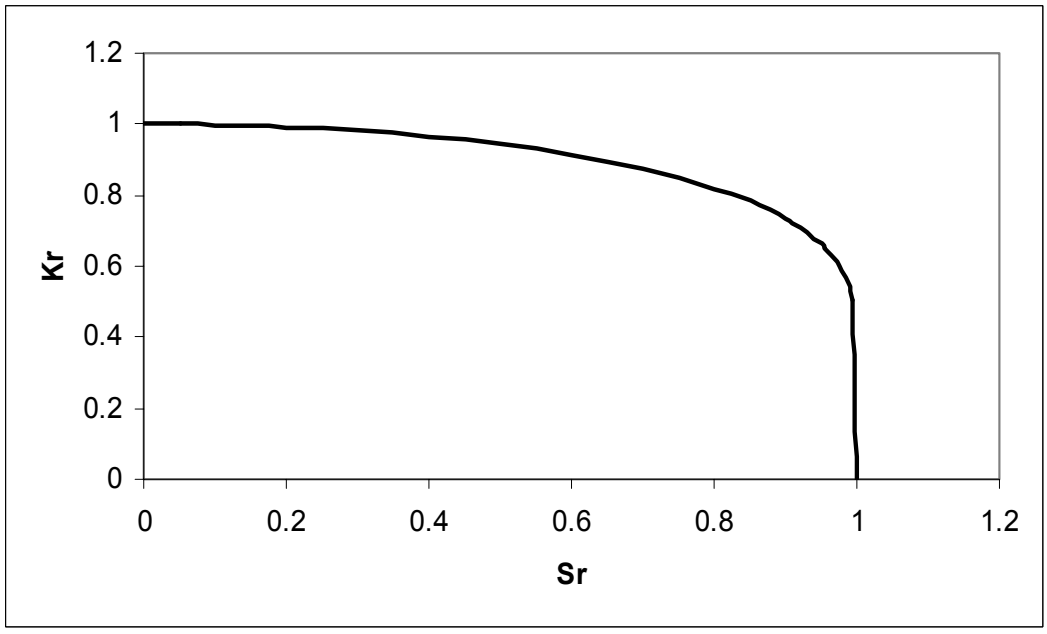

Figure 2 Original Failure Assessment Line

3.3 Plasticity Correction Term

No residual stresses were included and no plasticity correction term was used, hence $\rho = 0$.

3.4 The Stress State

In order to determine the reference stress, and stress intensity factors, it is first necessary to determine the stress field that would exist in the pipe at the location of the defect, if the defect was not present. This is referred to here as the undisturbed stress field.

3.4.1 The Undisturbed Stress Field

The section of pipeline containing the defect (dent/gouge) is considered to be straight and only subject to internal pressure loading. The two significant (principal) stress components are thus the hoop stress, σ_H and the axial stress, σ_A which are given by

$$\sigma_H = \frac{PR}{w} \tag{10}$$

and

$$\sigma_A = \nu \frac{PR}{w}. \tag{11}$$

Since Poison's Ratio, ν (assumed as 0.3 for steel), is less than unity, the maximum (principal) stress is equal to the hoop stress. Furthermore, assuming that the hoop stress acts uniformly across the pipewall, the maximum principal stress state, assuming that the defect is not present, can be expressed as

$$\sigma_m = \sigma_H \tag{12}$$

and

$$\sigma_b = 0, \tag{13}$$

where σ_m and σ_b are known as the membrane and bending components of the maximum principal stress state, respectively.

3.4.2 Effect of the Dent

The change in curvature due to the presence of the dent leads to a modification of the stress state and this is described by

$$\sigma_m = \sigma_H \left(1 - 1.8 \frac{D}{2R} \right) \tag{14}$$

and

$$\sigma_b = 10.2 \sigma_H \frac{R}{w} \frac{D}{2R}. \tag{15}$$

The dent was assumed not to cause any residual stress field.

3.4.3 Stress Categorisation

In order to determine the effect of the stress state on the structural integrity it is necessary to categorise the stresses as primary or secondary. In general, primary stresses are load controlled stresses that can cause failure by both plastic collapse and fracture. Secondary stresses are displacement controlled (constrained) stresses that can contribute towards failure by fracture but cannot cause plastic collapse.

For the present study the membrane stress in the dent is categorised as primary and the bending stress is categorised as secondary. This is a simplifying assumption that takes account of the re-rounding effect of the internal pressure. In reality the situation is more complex, as at low pressures the bending stress will be largely primary but reduces with re-rounding as the pressure increases, giving it some of the characteristics of a secondary stress. The complete stress state is thus represented by

$$\sigma_m^p = \sigma_H \left(1 - 1.8 \frac{D}{2R} \right), \tag{16}$$

$$\sigma_m^s = 0, \tag{17}$$

$$\sigma_b^p = 0 \tag{18}$$

and

$$\sigma_b^s = 10.2\,\sigma_H \frac{R}{w}\frac{D}{2R}, \tag{19}$$

where superscripts 'p' and 's' denote primary and secondary respectively. These stress components are used to determine the reference stress and the stress intensity factor in the following sections.

3.5 Reference Stress

The gouge is considered to lie in a plane that is normal to the direction of the maximum principal stress (i.e. along the axial direction of the pipe). The presence of the gouge causes a localised reduction in wall thickness. Based on a consideration of equilibrium of forces, it follows that there will be a localised increase in maximum principal stress. It is this localised increase in stress that may lead to failure due to plastic collapse. Since only primary stresses can cause plastic collapse, the reference stress is a function of the primary membrane stress and local geometry, and can be expressed in the form

$$\sigma_{ref} = \frac{\sigma_m^p (1 - a/Mw)}{(1 - a/w)}. \tag{20}$$

The factor, M, is the Folias factor, and takes account of the effect of the gouge length, L. It is given by:

$$\mathrm{M} = \left[1 + 0.26\left(\frac{\mathrm{L}}{\sqrt{\mathrm{Rw}}}\right)^2\right]^{\frac{1}{2}} \tag{21}$$

3.6 Stress Intensity Factor

The gouge is considered to be a rectangular ($a \times L$) sharp defect and the condition for fracture is determined only by the gouge depth and not the gouge length. This effectively assumes that the gouge is long compared to its depth and so can be treated as two dimensional. More complex models for the stress intensity factor that take account of the length are available in codes such as [6], [7] if required. Both membrane and bending stresses can contribute to fracture and hence the stress intensity factor may be expressed in the form,

$$K = (\sigma_m^p Y_m + \sigma_b^s Y_b)\sqrt{\pi a}, \tag{22}$$

where a is the gouge depth and $Y_m(a/w)$ and $Y_b(a/w)$ are normalised stress intensity compliance functions. For the present purpose, the functions $Y_m(a/w)$ and $Y_b(a/w)$ are given by the conservative expressions for an infinitely long (ie two dimensional) edge crack in a strip subject to remote tension and bending loads:

$$Y_m = 1.12 - 0.23(a/w) + 10.6(a/w)^2 - 21.7(a/w)^3 + 30.4(a/w)^4 \tag{23}$$

and

$$Y_b = 1.12 - 1.39(a/w) + 7.32(a/w)^2 - 13.1(a/w)^3 + 14.0(a/w)^4. \tag{24}$$

3.7 Flow Stress

With reference to equation (7), the flow stress is commonly obtained by assigning a value of 0.5 to λ. However, since for many steels the ratio σ_u / σ_y typically lies within the range (1.2 -1.3), the flow stress was defined as

$$\sigma_f = 1.15\sigma_y . \quad (25)$$

This is consistent with the definition used by Shannon [9] and for typical pipeline steels is close to the Battelle definition of SMYS + 10 ksi [10].

3.8 Fracture Toughness

With reference to equation (4) it was assumed that the constant B was equal to zero and linear regression analysis was used to determine the constants A and α using the 132 original test data points used to derive [2]. This resulted in

$$K_{mat} = 10.5C_v^{0.878} \text{ (MPa}\sqrt{\text{m}}\text{)}, \quad (26)$$

where C_v is expressed in Joules.

4 THE PROPOSED NEW LIMIT STATE FUNCTION

The new model described in this section is based on that described in Section 3 but includes a number of modifications. The purpose of the modifications is (i) to align the new limit state function to that currently used by the HSE and (ii) to take account of advances in fracture mechanics methodologies that have taken place since the original model was constructed.

4.1 The Damage

In addition to the dent and gouge, described in Section 3.1, it is further assumed here that a micro-crack is also introduced at the root of the gouge. The gouge is now idealised as a rounded feature with its own stress concentrating effect. The revised geometry is shown in Figure 1. A small micro-crack is present at the gouge, and the fracture mechanics model is applied to the micro-crack in the reduced section remaining under the gouge. The limit state function, described in this section, is thus used to determine the conditions for failure of a micro-crack of depth δ at the root of a gouge of depth a and length L located in a dent of depth D that is present in a pipeline having radius R, wall thickness w, yield strength σ_y, ultimate tensile strength, σ_u, Charpy toughness C_v and subject to internal pressure P.

4.2 The Failure Assessment Line

In accordance with [6] the proposed functional form for the failure assessment line, F is given by the material independent definition:

$$F = (1 + 0.5L_r^2)^{-1/2}(0.3 + 0.7\exp(-0.6L_r^6)) \quad , \quad L_r \le L_{r\max} \quad (27)$$

$$F = 0 \quad , \quad L_r > L_{r\max} ,$$

where the load ratio L_r is defined by

$$L_r = S_r \frac{\sigma_f}{\sigma_y} = \frac{\sigma_{ref}}{\sigma_y} \quad (28)$$

and $L_{r\max}$ is given by

$$L_{r\max} = \frac{\sigma_f}{\sigma_y} . \quad (29)$$

This modification to the failure assessment line takes account of work hardening properties of the steel. If a stress - strain curve is available for the material, an alternative formulation is given in [6] for a less conservative line, but this level of sophistication was not warranted for the available test data set.

4.3 The Plasticity Correction Term

The plasticity correction term ρ is given by

$$\rho = \rho_1 \quad , \quad L_r \le 0.8$$
$$\rho = 4\rho_1(1.05 - L_r) \quad , \quad 0.8 \le L_r \le 1.05 \qquad (30)$$
$$\rho = 0 \quad , \quad 1.05 \le L_r ,$$

In the above, ρ_1 is given by

$$\rho_1 = 0.1\left(\frac{K^s}{K^p / L_r}\right)^{0.714} - 0.007\left(\frac{K^s}{K^p / L_r}\right)^2 + 0.00003\left(\frac{K^s}{K^p / L_r}\right)^5 , \qquad (31)$$

where the primary and secondary stress intensity factors, K^p and K^s, respectively, are given by

$$K^p = K_m^p + K_b^p$$

and (32)

$$K^s = K_m^s + K_b^s .$$

4.4 The Stress State

4.4.1 The Undisturbed Stress Field

The stress field remote from the location of the dent and gouge is identical to that used in the original model and hence is described by equations (12) and (13).

4.4.2 Effect of the Dent

In addition to the effect of the change in curvature on the undisturbed stress field described above, it is also recognised here that the plastic deformation associated with the presence of the dent will result in a residual stress field. Using $D/2R$ as a simple measure of plastic deformation, and noting that the residual stresses are secondary, the following stress state is proposed;

$$\sigma_m^p = \sigma_H\left(1 - 1.8\frac{D}{2R}\right), \qquad (33)$$

$$\sigma_m^s = (1-\xi)\Phi\left(\frac{D}{2R}\right)\sigma_y , \qquad (34)$$

$$\sigma_b^p = 0 \qquad (35)$$

and

$$\sigma_b^s = 10.2\,\sigma_H \frac{R}{w}\frac{D}{2R} + \xi\Phi\left(\frac{D}{2R}\right)\sigma_y \qquad (36)$$

In the above ξ is a constant to be determined within the range 0 to 1 and Φ is a function of $D/2R$ given by

$$\Phi = \frac{D}{2R} \quad , \quad \frac{D}{2R} < \zeta$$

and (37)

$$\Phi = 1 \quad , \quad \frac{D}{2R} \ge \zeta ,$$

where ζ is a further constant to be determined.

4.5 Reference Stress

The effect of the micro-crack, on the susceptibility to plastic collapse, is to increase the effective depth of the gouge from a to $a+\delta$. The reference stress may thus be expressed as

$$\sigma_{ref} = \frac{\sigma_m^p[1-(a+\delta)/Mw]}{[1-(a+\delta)/w]}, \quad . \tag{38}$$

where σ_m^p is given by equation (33) and M is given by equation (21).

4.6 Stress Intensity Factor

In this case, the gouge is treated as blunt (not crack-like) and hence does not make a direct contribution to the stress intensity factor. However, there will be a localised increase in the stress at the root of the gouge (the location of the micro-crack) and this results in a modification of the stress state described by:

$$\sigma_m^p = \sigma_H\left(1-1.8\frac{D}{2R}\right)K_t, \tag{39}$$

$$\sigma_m^s = (1-\xi)\Phi\left(\frac{D}{2R}\right)\sigma_y, \tag{40}$$

$$\sigma_b^p = 0 \tag{41}$$

and

$$\sigma_b^s = 10.2\,\sigma_H\frac{R}{w}\frac{D}{2R}K_t + \xi\Phi\left(\frac{D}{2R}\right)\sigma_y, \tag{42}$$

where K_t is the notch stress concentration factor for a semi-elliptical notch [11] and is given by:

$$K_t = 1+2\sqrt{a/r}, \tag{43}$$

where *r* is the radius of the root of the gouge. The gouge radius is regarded as a further fit parameter here.

The stress intensity factor is then given by

$$K = [(\sigma_m^p+\sigma_m^s)Y_m(\delta/(w-a)) + \sigma_b^s Y_b(\delta/(w-a))]\sqrt{\pi\delta}, \tag{44}$$

where the relevant stress components are given by equation (39), (40) and (42) and the functions of Y_m and Y_b are given by equations (23) and (24) with the argument a/w replaced with $\delta/(w-a)$.

4.7 Flow Stress

The flow stress is taken to be the same as that used in the original model and hence is given by equation (25).

4.8 Fracture Toughness

The basic correlation between fracture toughness and Charpy Energy given by equation (3) is assumed here and the constants A, B and α are determined (along with other parameters) in the following section.

5 QUANTIFICATION OF NEW LIMIT STATE FUNCTION PARAMETERS

In addition to the parameters, A, B, α, ξ and ζ identified above, it is also necessary to determine the depth of the micro-crack δ. Evidence of micro-cracking was not sought at the time of the original testing since this element of the model was not conceived at that time. Consequently, no physical

measurements are currently available on which to base this quantity. It is therefore necessary to treat this quantity as a further 'fit' parameter.

Intuitively the depth of the micro-crack is likely to be dependent on the size of the remaining ligament and on the amount of plastic straining. Assuming that $D/2R$ is a simple measure of plastic strain, a relationship of the form,

$$\delta = C\left(\frac{a}{w}\right)^{\gamma}\left(\frac{D}{2R}\right)^{\beta} \quad , \tag{45}$$

is postulated, where C, γ and β are constants.

Hence, in order to complete the definition of the new limit state function it is necessary to assign values to the parameters, A, B, C, α, β, γ, ξ, ζ, and r.

In principle, although cumbersome, it would be possible to determine values for the above nine parameters, that would represent the best fit using non-linear regression analysis. However, such an approach would involve a level of analysis that is not warranted for the present purpose. Consequently a pragmatic approach was adopted. This involved iteratively assigning values to each of the nine parameters and visually observing the 'goodness of fit' of the data to the failure assessment line. In addition to the 'visual information' a check on the parameter,

$$\sum_i (K_{ri} - F(L_{ri}))^2 \, , \tag{46}$$

was made, where K_{ri} and L_{ri} are computed values for each of the i data.

It is important to note that 112 of the 132 tests were made on rings and only 20 were made on pressurised cylinders. The significance of this is that for the ring tests the length *L* can be regarded as tending to infinity in which case, as seen from equations (20) and (21), the effect of length is removed from the model. However, this is not considered to be a major limitation since length only appears in the reference stress formulation (21) and this aspect of the model is considered to be perfectly valid and will remain unchanged in the new model.

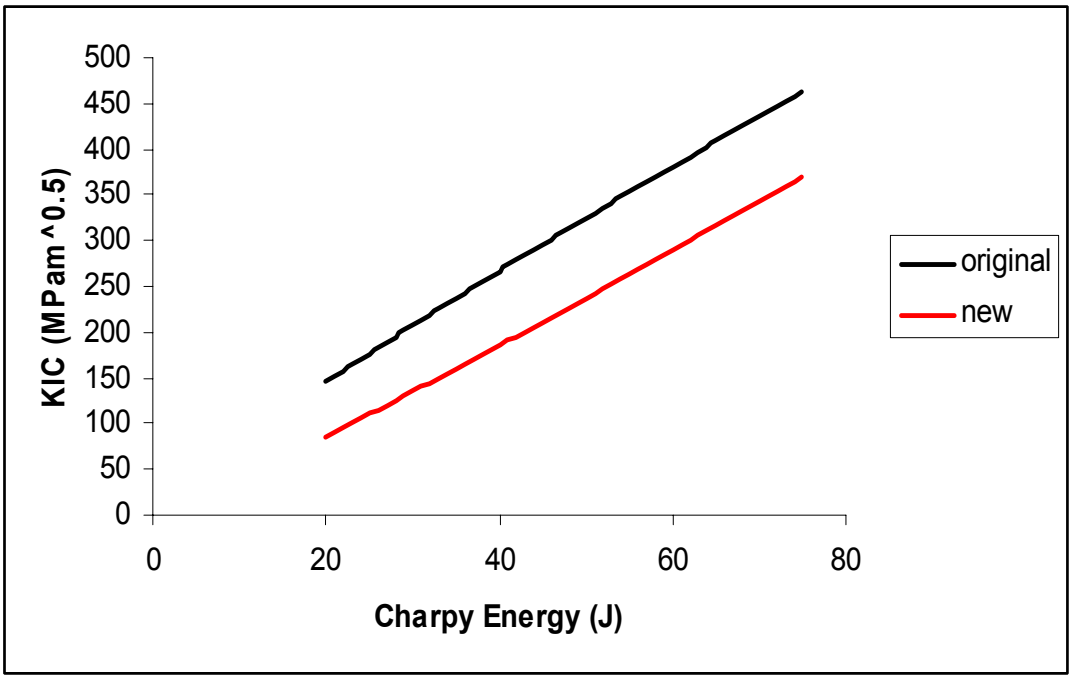

Figure 3 Correlation between Charpy impact energy and fracture toughness

5.1 Fracture Toughness

A range of values for *A, B* and *α* was investigated and the contribution of A was observed as the most sensitive parameter. The final outcome was $A = 3.2,\ B = 0$ and $\alpha = 1.1$. A comparison of this model with the original model is shown in Figure 3. The fracture toughness has generally reduced by a factor of about 0.7 and is regarded as being more representative of pipeline steels than the original model.

5.2 Micro-crack

The depth of micro-cracking plays a significant role and the final outcome was *C* = 0.023, β = 0.5 and *γ*= 1.5. The application of these values to the 132 test data points resulted in a mean value for *δ* of 0.4mm and a standard deviation of 0.2mm. These values are considered to be physically reasonable given the likely depth of a work hardened layer at the base of the gouge.

5.3 Residual Stress

The best fit was obtained for a very small value of $\zeta\ (\rightarrow 0)$ implying that a residual stress equal to the yield strength was appropriate to all situations. This is not too surprising since denting clearly introduces permanent plastic deformation. However, the fit was relatively insensitive to ξ indicating that treating the residual stress field as either membrane or bending makes little difference. In view of this a value of $\xi = 0$ (pure membrane) was arbitrarily chosen. Given the relatively shallow depth of the micro-crack compared to the remaining ligament, there would be little variation of a pure bending stress field over the micro-crack length. Hence there would be little difference between the effects of a membrane or a bending field for these shallow cracks. If the micro-crack were deeper, a greater difference might be expected.

5.4 Gouge Radius

Many of the tests were conducted using flat bottomed gouges. This would have resulted in an 'effective' gouge radius ($\rightarrow \infty$) that is greater than would be generally incurred in practice.

In practice, the gouge radius is likely to be determined by the size, shape and angle of incidence of the indenter and in general will be significantly greater than the gouge depth. For the present purpose the gouge radius was taken to be a fit parameter and a value of 0.2m was found to give a good fit. This 'large' value is consistent with the flat bottomed nature of the test geometries and is considered to be representative of gouge radii that will be encountered in the field.

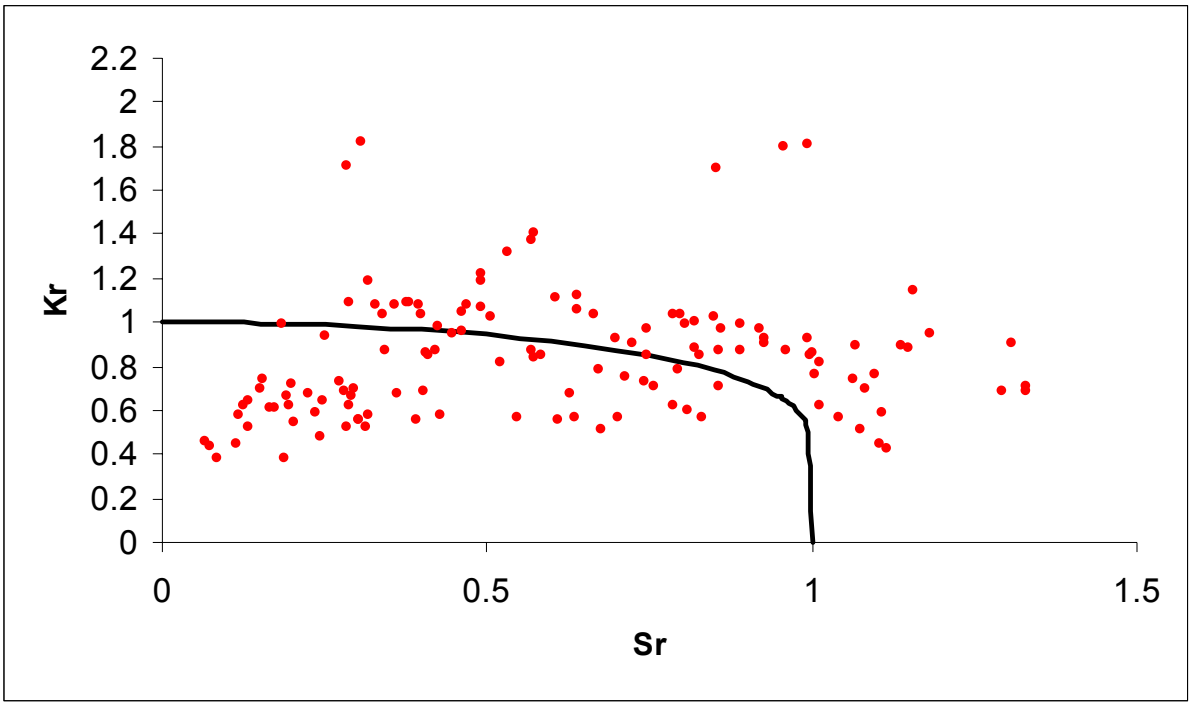

Figure 4 I Illustration of the data fitted using the original limit state function [2]

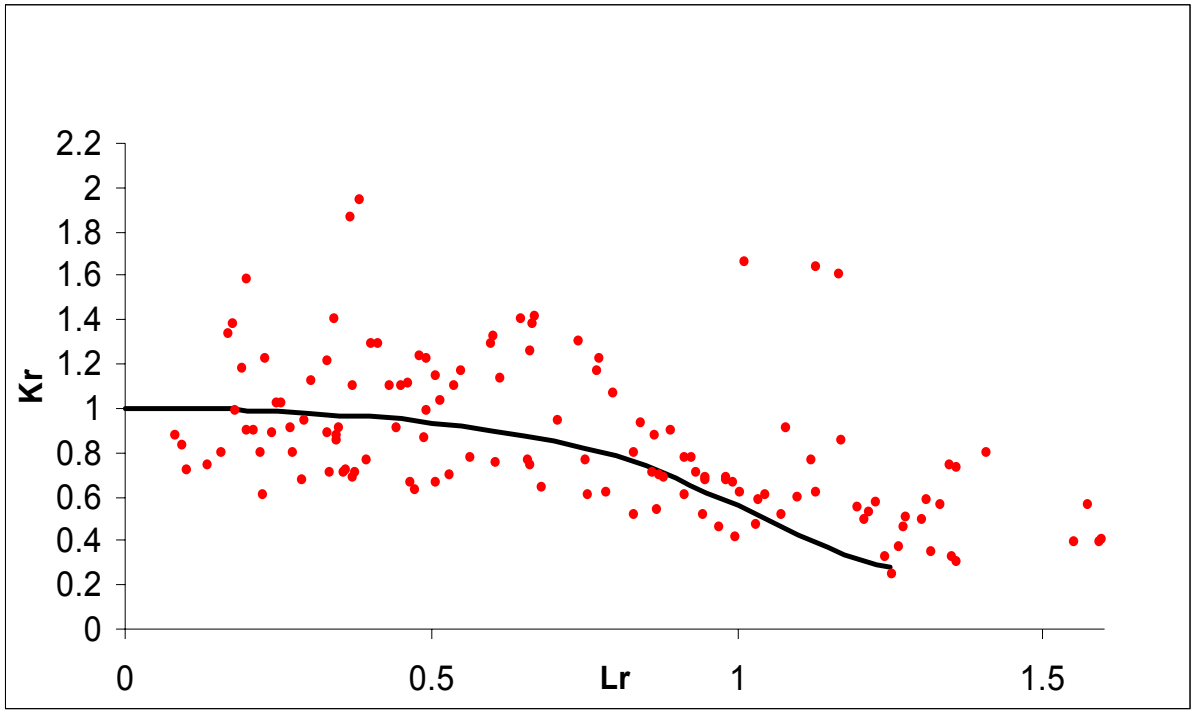

Figure 5 Illustration of the new limit state function using all test results.

5.5 New Limit State Function

The new limit state function is fully described by equations (3), (27-32) and (37-42) and the values of the parameters given above. A comparison of the fit of the new and original limit state functions to the test data is illustrated in Figures 4 and 5.

It can be seen from these figures, that although some scatter still remains in the new model, the improvement is significant. Notably, the general functional behaviour of the failure assessment line and the data are well aligned; no such behaviour can generally be seen using the original model shown in Figure 4. Some scatter about the failure assessment line is to be expected, as the analysis is intended to be "critical" rather than conservative. By using a model without a built-in safety factor the user has to take a decision on the safety factor required, or to use a reliability based approach to determine failure probabilities. The new model is thus considered to be a very significant improvement on the original model and consequently will provide a firmer basis for risk and integrity management.

A further point to note is that 20 of the 132 tests were made on pressurised cylinders (vessels) and not rings, as mentioned above. In the case of vessels both gouge depth and gouge length should be taken into account in accordance with equations (20) and (21). A significant effect of gouge length will be a reduction in the value of L_r. The four points at the extreme right of Figure 5 (and Figure 4) represent the outcomes of three of the vessel tests and consequently, since, the length was implicitly assumed to be infinite, have erroneously high L_r values. In order to obtain a more valid indication of the fit, the 20 vessel tests were removed and the revised plot is shown in Figure 6. The most notable change is the removal of the four points to the extreme right of Figure 6; the effect on the other 17 points appears to be less remarkable. Also for completeness a vertical line has been included that represents the value of $L_{r\max}$ (see equation (29)). Note that if measured defect length were known then the actual effect on the fit could be investigated. However, for the present purpose this level of detail is of no real significance.

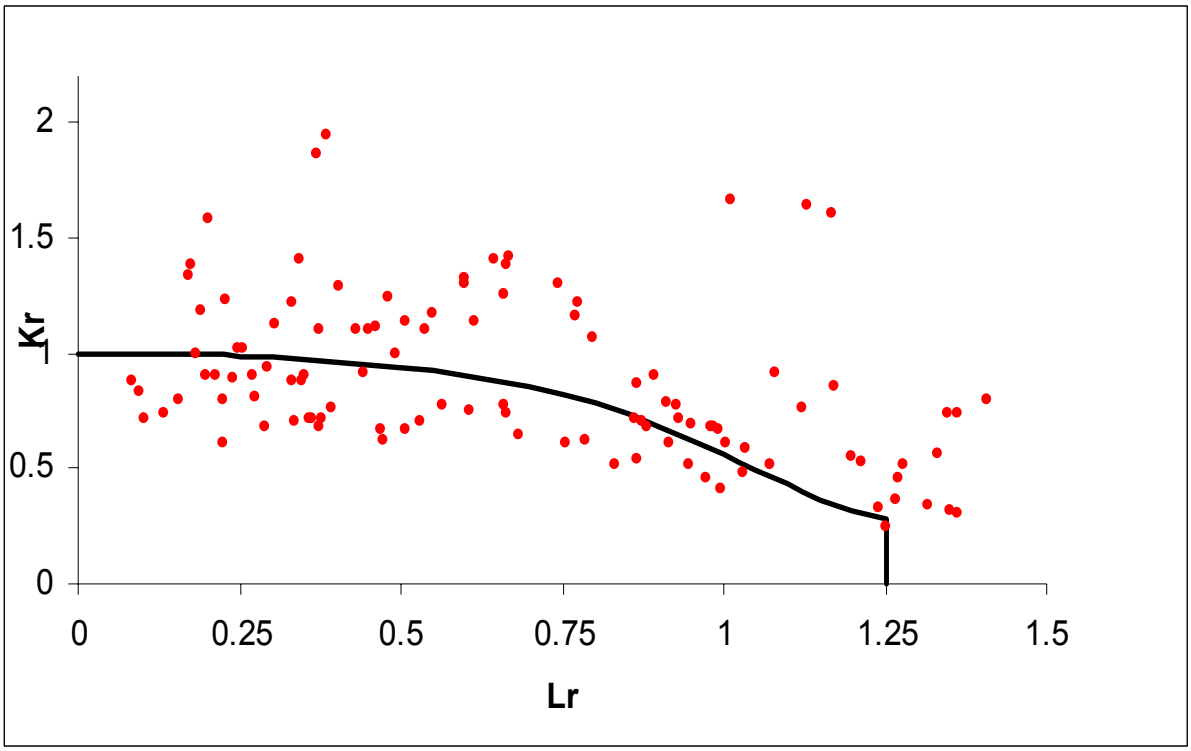

Figure 6 Illustration of the Data Fit using the new limit state function– ring expansion tests only

Also, a more detailed treatment of the fit through the use of non-linear regression, for instance, may result in some refinement of the values of the parameters. However, noting that the underlying test data set is 25 years old and subject to some uncertainty, such a refinement is not considered to be appropriate at the present stage. If more recent test data were included in the analysis a more detailed statistical treatment may be worthwhile.

Overall, the analysis presented has identified a number of shortcomings of the original model and has produced a revised model that is significantly more accurate. However, the semi-empirical nature of the model still remains. It is therefore recommended that more detailed theoretical study, building on the findings of this work and supported by more detailed testing should be undertaken in the near future. The model provides a framework to include more detailed effects such as time dependent material behaviour (delayed failure), the effect of pre-strain on the material properties [12] and better representation of the effect of dent geometry on the stresses acting on the gouge.

6 CONCLUSIONS

The salient features of the failure assessment line approach to elastic-plastic fracture mechanics have been briefly described.

The relationship between the fracture mechanics methodology and the existing limit state function developed in the early 1980s for assessing the significance of mechanical damage has been described in full detail.

A new limit state function has been derived taking account of enhancements to the elastic-plastic fracture mechanics methodology that have been introduced since the time that the original was developed.

In addition to the above enhancements, the new model includes the effects of residual stress and the presence of a micro-crack.

The new model has the same functional form as that used by HSE and is supported by a fit to the test data that were obtained at the time of the development of the original model.

7 ACKNOWLEDGEMENTS

This work was funded by the members of the United Kingdom Onshore Pipelines Association; this is gratefully acknowledged.

8 REFERENCES

[1] M.R. Acton, P.J. Baldwin, T.R. Baldwin & E.E.R. Jaeger, 'The Development of the PIPESAFE Risk Assessment Package for Gas Transmission Pipelines', IPC 98, Calgary, June 1998.

[2] P. Hopkins, 'The application of fitness for purpose methods to defects detected in offshore transmission pipelines', Welding and weld performance in the process industry. London: IBC Conferences 1992, pp1-49.

[3] R. J. Bood, M. R. Galli, U. Marewski, P. Roovers, M. Steiner & M. Zarea, 'EPRG methods for assessing the tolerance and resistance of pipelines to external damage', *3R International* 1999; Part 1: **38**(10-11) pp739-44; Part 2: **38**(12) pp806-11

[4] W. A. Maxey, 'Outside force defect behaviour'. Seventh symposium on line pipe research, Paper 14. Houston, October 14-16 1986. Arlington, Virginia: Pipeline Research Committee 1986, pp1-33.

[5] D. Linkens, N.K. Shetty & M. Bilo, 'A Probabilistic Approach to Fracture Assessment of Onshore Gas-Transmission Pipelines, Pipes & Pipelines International, July-August, 1998.

[6] R6 Revision 4, 'R6 Assessment of the Integrity of Structures Containing Defects', 2000, British energy plc

[7] BS 7910, 'Guide On Methods For Assessing The Acceptability Of Flaws In Metallic Structures', British Standards Institution, Incorporating amendment 1, 2000

[8] D.S. Dugdale, 'Yielding of Steel Plates Containing Slits', Journal of the Mechanics of Physics & Solids, Volume 8 pp 100-104,1960.

[9] R. W. E. Shannon, 'The failure behaviour of linepipe defects'. *International Journal of Pressure Vessels and Piping* 1974;**2**:243-55.

[10] J. F. Kiefner, W. A. Maxey, R. J. Eiber and A. R. Duffy, 'Failure stress levels of flaws in pressurized cylinders'. Progress in flaw growth and fracture toughness testing ASTM STP 536. Philadelphia: American Society for Testing and Materials 1973, pp461-81.

[11] R. E. Peterson, 'Stress concentration factors'. New York: Wiley; 1974.

[12] A. Cosham, 'A model of pre-strain effects on fracture toughness'. *Journal of Offshore Mechanics and Arctic Engineering* 2001;**123**:182-90.